Advanced Undergraduate-Laboratory Experiment on Electron Spin Resonance in Single-Crystal Ruby

Lee A. Collins, Michael A. Morrison and Paul L. Donoho

Citation: American Journal of Physics **42**, 560 (1974); doi: 10.1119/1.1987777
View online: https://doi.org/10.1119/1.1987777
View Table of Contents: https://aapt.scitation.org/toc/ajp/42/7
Published by the American Association of Physics Teachers

Advanced Undergraduate-Laboratory Experiment on Electron Spin Resonance in Single-Crystal Ruby*

LEE A. COLLINS
MICHAEL A. MORRISON
PAUL L. DONOHO
Department of Physics
William Marsh Rice University
Houston, Texas 77001
(Received 16 August 1972; revised 27 July 1973)

An electron-spin-resonance experiment which has been successfully performed in the advanced undergraduate laboratory at Rice University is described. In this experiment, the ESR spectrum arising from Cr^{3+} ions in a single-crystal synthetic ruby is studied. Both the positions and the intensities of the observable resonance lines are measured, and the data are compared to the predictions of a theory based upon the use of a simple, effective-spin Hamiltonian for the Cr^{3+} ion. Although this experiment requires the use of apparatus not always available in undergraduate laboratories, it involves measurements on a quantum-mechanical system whose behavior, although far from trivial, is, nevertheless, simple enough that the correspondence between observable physical quantities and their theoretically predicted values can be convincingly demonstrated. Since the student who undertakes this experiment can carry out himself all the measurements and perform for himself all the calculations required for interpretation of the experimental results, the excellent agreement between the theory and the experiment is demonstrated for the student in a vivid fashion. The complete execution of the experiment, including the full theoretical analysis of the problem, is very helpful to the student in his attempt to grasp the significance of the many new quantum-mechanical quantities to which he is being exposed in his undergraduate studies.

I. INTRODUCTION

This paper describes an experiment on electron spin resonance (ESR) in a single-crystal ruby which has been carried out over a period of several years in the advanced undergraduate physics laboratory at Rice University. In this experiment, the student learns some of the techniques pertinent to an active area of modern research, but, more importantly, he has an opportunity to see, often for the first time, a convincing demonstration of the agreement between his experimental results and the predictions of a rather abstract quantum-mechanical formulation of the problem. The physics curriculum at Rice includes a two-year, four-semester sequence of courses in quantum mechanics and its applications in many areas of modern physics. Beginning in the junior year, this curriculum introduces the student to many topics previously found in graduate-level courses. In view of the much greater depth of the new curriculum, experiments have been sought for the accompanying advanced laboratory which will deal with the concepts included in the lecture courses in such a way as to stimulate the interest of the student in quantum mechanics and give him more confidence in his understanding of it. The experiment described here represents one successful way of accomplishing this goal.

The phenomenon of electron spin resonance is quite useful pedagogically as an example of a quantum-mechanical system possessing a small number of energy levels among which transitions can be readily induced. The introductory literature on ESR up to 1965 is listed in a recent resource letter[1] which is quite useful to the student beginning this experiment or a similar one. In the present experiment, emphasis is placed upon the physics underlying the observed phenomena rather than on the actual experimental technique, in the same manner as in the earlier work described by Limon and Webb.[2] It is not the purpose of the present paper to explain the fundamental phenomena of magnetic resonance, which are treated quite well in many of the references of the resource letter.[1] Rather, an attempt is made here to show how ESR measurements can be used to obtain information about the quantities which characterize the quantum-mechanical behavior of a paramagnetic system of ions in a crystal lattice. Although the behavior of an ion in a crystalline environment may be quite compli-

cated, the characteristics of the energy levels near the ground state are often described quite accurately through the use of a spin Hamiltonian, a quantum-mechanical operator which is constructed in such a way that it can be used to predict the dependence of the energy levels of the ion on the strength of an applied magnetic field. Although the complete theory of the spin Hamiltonian is beyond the scope of this paper, it will be seen in the following sections that a spin Hamiltonian can be plausibly developed for the case of interest, the Cr^{3+} ion in a ruby crystal. This spin Hamiltonian will accurately describe the dependence of both the energy levels of the ion and the magnetic-dipole transition probabilities for transitions between these levels on the magnitude and direction of the applied magnetic field.

In the experiment described here, the Cr^{3+} ion in ruby was chosen as the system whose ESR spectrum was to be investigated for several reasons. First, large resonance signals can be obtained with the sample at room temperature; thus, neither a cryogenic system nor a highly sensitive spectrometer is required. Second, large, single-crystal specimens of synthetic ruby can be obtained at low cost, and their crystallographic axes can be easily determined by either optical or x-ray methods. Third, the ESR spectrum is composed of several well-separated resonance lines, depending upon the direction of the magnetic field, making the system much more interesting than, for example a simple, free-radical system. This spectrum is split only by direct crystal-field effects, avoiding the added complications of hyperfine splitting. The spectrum, although not simple, can nevertheless be analyzed by the beginning student. Finally, the dependence of the various line intensities provides an interesting illustration of the magnetic-dipole selection rules.

The experiment has been carried out by a total of approximately 50 students over a period of several years. These students have usually worked together in groups of two or three, under the supervision of one of the authors (P.L.D.). The description of the details of the experiment given here is due primarily to two of the authors (L.A.C. and M.A.M.), who were undergraduates majoring in physics at the time they performed the experiment. Although the experimental details given here concern the particular set of apparatus in the laboratories at Rice University, it is quite possible to perform this experiment with much less elaborate equipment, and some of the ways in which the experimental procedure can be simplified are pointed out where appropriate.

The student undertaking this experiment is provided with a certain amount of introductory lecture material concerning the fundamentals of magnetic resonance at the level given by several authors.[3–7] It is assumed that he also has an acquaintance with quantum mechanics at the level of the text, *Principles of Modern Physics*, by Leighton.[8] In the remainder of this paper, it is therefore assumed that the reader is thoroughly familiar with these fundamental concepts, and the emphasis is placed on a description of that part of the theory of magnetic resonance necessary for the understanding of the experiment described here.

II. DEVELOPMENT OF THE SPIN HAMILTONIAN FOR Cr^{3+} IONS IN Al_2O_3

The system of interest, whose energy levels are to be studied by the method of ESR, is the trivalent chromium ion, substituted into the α-Al_2O_3 (corundum) lattice in a normal aluminum site. The situation is depicted schematically in Fig. 1, where the trigonal symmetry of the environment of an aluminum or chromium ion can be seen. The free Cr^{3+} ion has a ground-state multiplet described in Russell–Saunders notation as $^4F_{3/2}$. That is, the orbital angular momentum is $L=3$, the spin is $S=\frac{3}{2}$, and the total angular momentum is $J=\frac{3}{2}$. This ground-state multiplet arises from an electronic configuration consisting of three $3d$ electrons. The Cr^{3+} ion, however, when situated in the Al_2O_3 lattice, is subjected to a strong electric field due to the neighboring lattice ions. It is not possible in this paper to discuss in detail the full theory of the crystalline electric field, but a simple physical description of its effects can be given for the present case.

The $3d$ electrons of the Cr^{3+} ion are strongly repelled by the negative oxygen ions which surround the chromium site. The normally sevenfold, degenerate, ground orbital states corresponding to the $2L+1$ orbital states for $L=3$ are no longer eigenstates of the ionic Hamiltonian, which now includes the potential due to the crystalline electric field. Instead, the electrons take on a configuration in which the ground state

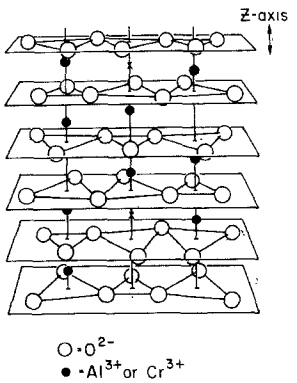

FIG. 1. Pictorial view of α-Al_2O_3 lattice, showing z axis and ionic sites.

is one which minimizes the average value of the crystalline potential energy. For the present case, this ground state is nondegenerate and, since the first excited orbital state is approximately 1 eV higher in energy,[6] the ground orbital state is the only one populated at normal temperatures. The crystalline electric field has, however, little effect on the electronic spins, the only effect being an indirect one through the mechanism of spin–orbit coupling. Thus, the ground orbital state will retain its four-fold spin degeneracy, except for a very small splitting of the spin levels due to spin–orbit coupling. These spin levels are the subject of interest in the ESR problem discussed here.

It is possible to regard these spin states associated with the ground orbital state as an isolated set of states which, neglecting the small crystal-field splitting discussed below, can be regarded simply as the eigenstates of a free spin angular momentum of quantum number $S = \frac{3}{2}$. The effect of the crystalline electric field is a small splitting in energy of the levels corresponding to $m = \pm\frac{1}{2}$ from those corresponding to $m = \pm\frac{3}{2}$. This splitting into two doublets, which is very much smaller than the separation of the orbital levels, is called the "zero-field" splitting, signifying that it is a splitting of the ground-state spin multiplet which occurs in the absence of an applied magnetic field. The application of a magnetic field will lead, then, to the normal Zeeman splitting of the two doublets, with the general result that the ground-state spin multiplet will be split into four states of different energies. It is the total behavior of the four spin levels of the Cr^{3+} ion, under the combined effects of both the crystalline electric field and the applied magnetic field, that is the concern of this section.

If the four spin states are considered to be the usual angular-momentum eigenstates of the square of the spin S^2, and the z component of the spin S_z, characterized by quantum numbers $S = \frac{3}{2}$ and $m = \frac{3}{2}, \frac{1}{2}, -\frac{1}{2}, -\frac{3}{2}$, then it is possible to construct relatively simple spin operators which will describe accurately the separate effects of the crystal field and the applied magnetic field. Consider first the effect of the crystal field, which produces a splitting of the four states into two doublets. The following operator can be used to describe this splitting:

$$\mathcal{H}_C = -D(S_z^2 - \tfrac{5}{4}). \tag{1}$$

Since the original eigenstates are eigenstates of S_z, they are simultaneously eigenstates of S_z^2, with eigenvalues for E_C given by

$$E_C = -D(m^2 - \tfrac{5}{4}). \tag{2}$$

Thus, when $m = \pm\frac{1}{2}$, E_C equals $+D$, and when $m = \pm\frac{3}{2}$, E_C equals $-D$, with a total zero-field splitting equal to $2D$ between the two doublets. It should be pointed out that the choice of the z axis is no longer arbitrary; this axis must coincide with the crystallographic c axis shown in Fig. 1 for reasons associated with the rotational symmetry of the crystal field. The form of $\mathcal{H}_C$ given in Eq. (1) can be predicted through the use of a more thorough theory of the crystal field,[6] but such a derivation is beyond the scope of this paper.

The effect of the applied magnetic field may also be considered separately, ignoring for the moment the zero-field splitting. The magnetic field will produce the normal Zeeman splitting of the four energy levels, and its effect may be described by the usual Zeeman interaction Hamiltonian:

$$\mathcal{H}_Z = g\mu_B \mathbf{H} \cdot \mathbf{S}. \tag{3}$$

In this expression, g is the Landé spectroscopic splitting factor, which would be equal to approximately 2 for a free spin. The presence of the crystal field modifies the g value slightly, how-

ever, through the indirect effect of the spin–orbit coupling, changing its magnitude somewhat and converting it into a tensor quantity with different values depending upon whether the applied field is parallel to the c axis or perpendicular to it. In the present case, however, the non-scalar nature of the g tensor is unimportant, and it is assumed in what follows that Eq. (3) adequately represents the Zeeman interaction, with the actual value of g to be determined experimentally. The quantity μ_B is, of course, the Bohr magneton. Thus, if there is no zero-field splitting of the spin levels, the Zeeman Hamiltonian would lead to energy levels given by $E_Z = g\mu_B Hm$. In the above equations and in the remainder of this paper energies are expressed in frequency units, the "natural" units for resonance problems, as discussed in Appendix I.

Two questions now arise: First, can the two Hamiltonian operators $\mathcal{H}_C$ and $\mathcal{H}_Z$, constructed specifically to account for two independent physical interactions, be combined to give an effective Hamiltonian operator which will accurately describe the dependence of the energy levels on the applied magnetic field in the presence of the crystalline electric field? Second, will this total resultant spin Hamiltonian, as it is called, lead to the correct prediction of transition probabilities for transitions induced between pairs of levels by the rf magnetic field normally used to produce magnetic resonance? The answer to both questions is affirmative; the two terms which describe separately the effects of the magnetic field and the crystalline electric field can be added to produce a resultant spin Hamiltonian which provides a complete description of all aspects of the static and dynamic behavior of the four spin levels under the application of both static and time-dependent magnetic fields.

In the experiment described in the following sections of this paper, both the transition frequencies (energy differences) and the relative transition probabilities for ESR transitions between several pairs of the spin levels are measured. From these measurements, it is possible to determine the two main parameters of the spin Hamiltonian, g and D, and it is possible to confirm that the spin Hamiltonian, $\mathcal{H}_S = \mathcal{H}_C + \mathcal{H}_Z$, does lead to a quantitatively correct description of all the observations which can be made in an ESR experiment on this system. Before beginning a description of the experimental work and its results, it is appropriate to carry out an analysis of the problem of the calculation of the energy levels of the spin system resulting from the assumed form for the spin Hamiltonian and the determination of transition frequencies and transition probabilities. Thus, the problem of finding the eigenstates and eigenvalues of the spin Hamiltonian, a procedure usually referred to as the diagonalization of the spin Hamiltonian, is undertaken at this point.

III. DIAGONALIZATION OF THE SPIN HAMILTONIAN

It is necessary to find the eigenvalues and eigenvectors of the following operator, which has been designated as the spin Hamiltonian:

$$\mathcal{H}_S = g\mu_B \mathbf{H}\cdot\mathbf{S} - D(S_z^2 - \tfrac{5}{4}). \tag{4}$$

It is assumed that the quantities g and D have definite values, but that these values must be determined from experimental measurements. Consider first the determination of these quantities. The spin Hamiltonian is readily diagonalized in the special case in which the magnetic field is directed along the z axis, since in this case the spin Hamiltonian is simply a function of S_z, and the eigenvalues are simply obtained by replacing S_z with the four values of the quantum number m in the spin Hamiltonian:

$$E_m = g\mu_B H_z m - D(m^2 - \tfrac{5}{4}). \tag{5}$$

The eigenvectors of the spin Hamiltonian for this special case, the eigenvectors of S_z, are denoted in the Dirac ket notation as $|\, m\rangle$ and, of course, for the present case, m takes the values $\frac{3}{2}$, $\frac{1}{2}$, $-\frac{1}{2}$, and $-\frac{3}{2}$. The linear dependence of the energies on the applied field is depicted in Fig. 2, where some of the allowed magnetic-dipole transitions, for which $\Delta m = \pm 1$, are also indicated. This magnetic-dipole selection rule arises in the usual manner from consideration of the transition probability for transitions between levels induced by an oscillating small magnetic field perpendicular to the large applied static field. Since the transition probabilities are also of interest in the more general case in which the field is not parallel to the

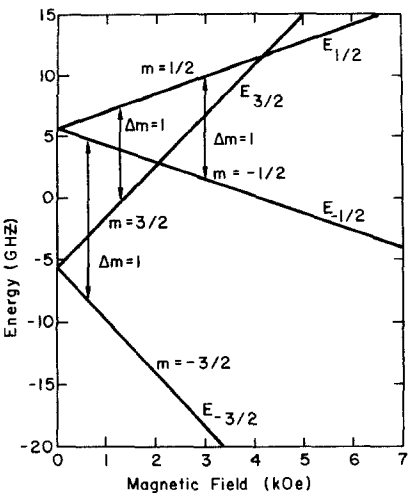

FIG. 2. Field dependence of Cr^{3+} spin levels with field along z axis.

z axis, it is useful to review the method for calculating transition probabilities and determining selection rules for this special case.

The "Fermi Golden Rule" for transition probabilities between two states, i and j, can be written[5]

$$W_{ij}=(1/\hbar^2)\mid\langle i\mid g\mu_B H_y S_y\mid j\rangle\mid^2 f(\nu-\nu_{ij}), \quad (6)$$

where it is assumed that a small oscillating field of amplitude H_y is applied along the y axis at frequency ν and that the transition frequency between the two states is $\nu_{ij}=(E_i-E_j)/h$. The function $f(\nu-\nu_{ij})$ is a line-shape function whose origin and detailed nature are not important for the present discussion. The transition probability is zero unless the matrix element of S_y is different from zero. It is well known that this operator S_y possesses non-zero matrix elements between the eigenstates of S_z only if the m values of the states differ by ±1; hence the magnetic-dipole selection rule. Only those transitions for which the magnetic-dipole selection rule is obeyed will be observed in the usual ESR experiment. Thus, with the field along the z axis, the transitions of interest are those illustrated in Fig. 2, namely: $\frac{3}{2}\rightarrow\frac{1}{2}$, $\frac{1}{2}\rightarrow-\frac{1}{2}$, and $-\frac{1}{2}\rightarrow-\frac{3}{2}$. The transition energies for these allowed transitions are the following:

$$E(\tfrac{3}{2}\rightarrow\tfrac{1}{2})=\pm\mid 2D-g\mu_B H_z\mid, \quad (7)$$

$$E(\tfrac{1}{2}\rightarrow-\tfrac{1}{2})=\pm g\mu_B H_z, \quad (8)$$

$$E(-\tfrac{1}{2}\rightarrow-\tfrac{3}{2})=\pm\mid 2D+g\mu_B H_z\mid. \quad (9)$$

Obviously, if the frequency ν at which the resonance is observed is less than $2D$, the $-\frac{1}{2}\rightarrow-\frac{3}{2}$ transition cannot be observed. Since in the present case $2D=11.46$ GHz,[9] a value greater than the frequency at which this experiment was performed, only the two transitions with energy differences given by Eqs. (7–8) are of interest. These two transitions will give rise to three observable resonances, occurring at different values of the applied field:

$$H_1=(2D-\nu)/g\mu_B,$$

$$H_2=\nu/g\mu_B,$$

$$H_3=(2D+\nu)/g\mu_B. \quad (10)$$

A measurement of H_2 permits the determination of g, and measurement of H_1 and H_3 permits the determination of the zero-field splitting constant D. Once g and D have been determined, the spin Hamiltonian may be diagonalized for any arbitrary direction of the applied field.

One problem arises in the attempt to apply the above analysis to the determination of g and D: How can it be established that the applied field lies exactly along the crystallographic z axis? Although the crystal may be accurately oriented by x-ray methods, it is usually difficult to place the crystal inside the resonant cavity of the microwave spectrometer in such a way that the orientation remains accurately known. If the field is not applied exactly along the z axis, of course, the above analysis leading to a means for the experimental determination of g and D is no longer valid. Thus, it is important to find a means for the determination of the exact direction of the crystallographic z axis with respect to the direction of the magnetic field when the specimen is in place in the spectrometer. An analysis of the results of the complete diagonalization of the spin Hamiltonian for an arbitrary direction of the applied field reveals, fortunately, a very accurate method for the determination of the direction of the z axis.

It is necessary, therefore, to proceed with the problem of the complete diagonalization of the spin Hamiltonian for the general case in which the field is directed at an angle θ to the z axis. There is no loss in generality if the field is assumed

to lie in the x–z plane, in which case the spin Hamiltonian takes the form

$$\mathcal{H}_S = g\mu_B H(S_z\cos\theta + S_x\sin\theta) - D(S_z^2 - \tfrac{5}{4}). \quad (11)$$

In contrast to the case in which the field was parallel to the z axis, the presence of the operator S_x in the spin Hamiltonian means that $\mathcal{H}_S$ is no longer diagonal in a representation whose basis vectors are the eigenvectors of S_z.

The simplest way in which to effect the complete diagonalization of the spin Hamiltonian lies in the use of matrix techniques, in which the eigenvectors are represented as column matrices and the Hamiltonian or any other operator is represented as a square matrix. The eigenvectors of the spin Hamiltonian will be denoted by Φ_n, where n is a label taking the values 1, 2, 3, and 4. The eigenvectors of S_z will be denoted by $|\,i\rangle$, where i is a label taking also the values 1, 2, 3, and 4, such that $i=1$ corresponds to $m=\frac{3}{2}$, etc. With this notation, the eigenvectors of the spin Hamiltonian can be written:

$$\Phi_n = A_{n1}|\,1\rangle + A_{n2}|\,2\rangle + A_{n3}|\,3\rangle + A_{n4}|\,4\rangle. \quad (12)$$

For each eigenvector Φ_n, there is, of course, a corresponding eigenvalue E_n. The matrix eigenvalue equation is then the following:

$$\begin{pmatrix} \langle 1|\mathcal{H}_S|1\rangle & \langle 1|\mathcal{H}_S|2\rangle & \langle 1|\mathcal{H}_S|3\rangle & \langle 1|\mathcal{H}_S|4\rangle \\ \langle 2|\mathcal{H}_S|1\rangle & \langle 2|\mathcal{H}_S|2\rangle & \langle 2|\mathcal{H}_S|3\rangle & \langle 2|\mathcal{H}_S|4\rangle \\ \langle 3|\mathcal{H}_S|1\rangle & \langle 3|\mathcal{H}_S|2\rangle & \langle 3|\mathcal{H}_S|3\rangle & \langle 3|\mathcal{H}_S|4\rangle \\ \langle 4|\mathcal{H}_S|1\rangle & \langle 4|\mathcal{H}_S|2\rangle & \langle 4|\mathcal{H}_S|3\rangle & \langle 4|\mathcal{H}_S|4\rangle \end{pmatrix} \begin{pmatrix} A_{n1} \\ A_{n2} \\ A_{n3} \\ A_{n4} \end{pmatrix} = E_n \begin{pmatrix} A_{n1} \\ A_{n2} \\ A_{n3} \\ A_{n4} \end{pmatrix}. \quad (13)$$

This matrix equation may be most easily worked out in terms of the matrices for the individual spin operators, S_x, S_z, and S_z^2, which can be found in many introductory books on quantum mechanics or worked out easily in terms of the operators S_z, S_+, and S_-. The explicit form for the matrix eigenvalue equation then becomes the following:

$$\begin{pmatrix} 3C/2-D-E_n & \sqrt{3}\,S/2 & 0 & 0 \\ \sqrt{3}\,S/2 & C/2+D-E_n & S & 0 \\ 0 & S & -C/2+D-E_n & \sqrt{3}\,S/2 \\ 0 & 0 & \sqrt{3}\,S/2 & -3C/2-D-E_n \end{pmatrix} \begin{pmatrix} A_{n1} \\ A_{n2} \\ A_{n3} \\ A_{n4} \end{pmatrix} = 0. \quad (14)$$

In Eq. (14), the abbreviations $C=g\mu_B H\cos\theta$ and $S=g\mu_B H\sin\theta$ have been used. The solution of the eigenvalue problem now consists of the determination of the four energies E_n which satisfy the above equation and the determination of the corresponding A_{ni}.

In order to solve the set of linear homogeneous equations represented by Eq. (14), it is necessary that the determinant of the matrix given in that equation be zero. This requirement leads to the secular equation

$$\begin{aligned} E_n^4 - E_n^2[2D^2 + 5(g\mu_B H)^2/2] \\ + 2DE_n(g\mu_B H)^2(3\cos^2\theta - 1) \\ + D^4 + 9(g\mu_B H)^4/16 \\ + D^2(g\mu_B H)^2(1 - 6\cos^2\theta)/2 = 0. \end{aligned} \quad (15)$$

This quartic equation has four roots, the four allowed values of E_n. Since the secular equation arises from a Hermitian matrix, the roots are all

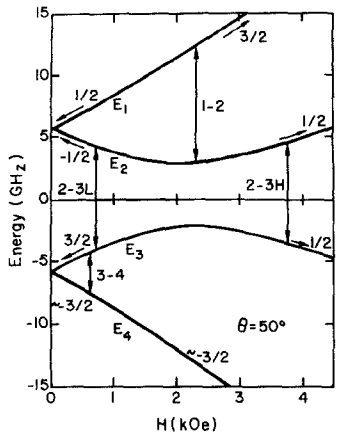

FIG. 3. Field dependence of Cr^{3+} spin levels with field at 50° from z axis.

guaranteed to be real, although they may not be distinct. Although standard algebraic solutions for quartic equations may be found in algebra texts, the solution of this equation is particularly simple if a numerical result is desired. Methods for the numerical solution of the secular equation using a digital computer are discussed in Appendix II. Once the E_n have all been found for a particular choice of H and θ, the coefficients A_{ni} can also be evaluated, as discussed in Appendix II.

An example of the dependence of the energy levels on the magnitude of the applied field is shown in Fig. 3, for $\theta=50°$. The energy levels are numbered arbitrarily, with E_1 referring to the level of highest energy and E_4 to the level of lowest energy. In Fig. 3 it can be seen that the field dependence of each level approaches the same slope as that of a level characterized by a pure m value at both low and high values of the applied field. For example, the slope of E_1 at low fields is that of a pure level with $m=\frac{1}{2}$, whereas for high fields it is the same as that of a pure level with $m=\frac{3}{2}$. This low-field and high-field behavior is indicated in Fig. 3. It should be pointed out that the notation used by some authors[9] to describe the levels makes use of the high-field effective value of m instead of the arbitrary labeling used here.

If the coefficients A_{ni} are examined, it will be seen that they depend strongly upon the magnitude and direction of the applied field, so that each level changes its composition in terms of the eigenstates of S_z as the magnitude or direction of the field is varied. Thus, it would be expected that the transition probability for a transition between two levels induced by an oscillating magnetic field perpendicular to the static field would also change as the field magnitude or direction varies. If the static field lies in the x–z plane, as previously assumed, then it is of interest to compute the transition probability induced by an rf field along the y axis. In this case, the relevant matrix element for a transition between levels j and k is the following:

$$\langle j \mid S_y \mid k \rangle$$
$$= i[(\sqrt{3}/2)(A_{j2}^* A_{k1} - A_{j1}^* A_{k2} + A_{j4}^* A_{k3} - A_{j3}^* A_{k4}) + A_{j3}^* A_{k2} - A_{j2}^* A_{k3}]. \quad (16)$$

The transition probability is, of course, proportional to the absolute square of the matrix element.

In an ESR experiment, the frequency at which resonance is observed is normally held constant while the magnetic field is varied through the condition for resonance. Curves showing the dependence of the individual energy levels on the magnitude of the field, such as those of Figs. 2 and 3, are not, therefore, particularly useful in

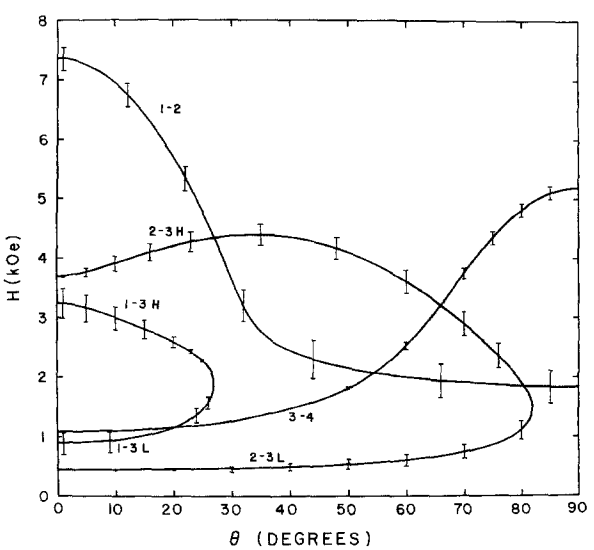

FIG. 4. Isofrequency plot of field vs angle for observable transitions at frequency of 9.0 GHz. Relative transition probabilities indicated.

the interpretation of experimental data or in the prediction of the field at which a particular transition will occur. It is worthwhile, therefore, to construct an isofrequency plot which will show for each transition of interest the magnitude of the field at which resonance occurs as a function of the direction of the field. Examples of such plots are illustrated in Figs. 4 and 5 for the present case, using the accepted values for g and D as given by Schulz–Dubois.[9] Included in these plots is information concerning the relative transition probabilities for the various transitions [shown as vertical bars whose length is proportional to the absolute square of the transition matrix element given in Eq. (16)]. The method for the computation of these isofrequency plots is outlined in Appendix III.

In Fig. 4, corresponding to a frequency of 9.0 GHz, it can be seen that the 1–2 transition can be observed at all angles, and that the transition probability is appreciable at all angles. At $\theta=0°$ this transition occurs at the field H_3, defined in Eq. (10). The 2–3 transition exhibits two branches, a low-field branch designated 2–3L and a high-field branch designated 2–3H. At 9.0 GHz this transition can be observed only for angles less than approximately 85°, whereas it can be observed at all angles at 10.0 GHz. For both branches, the transition probability is zero at $\theta=0°$, but for the high-field branch it increases rapidly as θ increases. It is this rapid variation of the transition probability for the 2–3H transition near $\theta=0°$ which permits the determination of the parallelism of the z axis of the crystal and the magnetic field. At $\theta=0°$, the transition is pure $\frac{3}{2}\rightarrow-\frac{1}{2}$, for which $\Delta m=2$, but as θ increases, the formerly pure $\frac{3}{2}$ level acquires a component with $m=\frac{1}{2}$, and the $-\frac{1}{2}$ level acquires a component with $m=-\frac{1}{2}$, making possible weak transitions for which the selection rule is obeyed.

The 1–3 transition also exhibits two branches at the frequencies of Figs. 4–5. At 0°, the resonance fields for the 1–3L and 1–3H transitions are, respectively, the fields H_1 and H_2 defined in Eq. (10). The 3–4 transition is observable at all angles at any frequency, but the transition probability is so small for angles less than approximately 40° that the transition is normally difficult to detect experimentally at small angles.

Many more isofrequency plots are presented in the paper by Schulz–Dubois.[9] In that paper, account is taken of the anisotropic nature of the g factor in the spin Hamiltonian, although the anisotropy is so small that it is difficult to measure (and it has been ignored here).

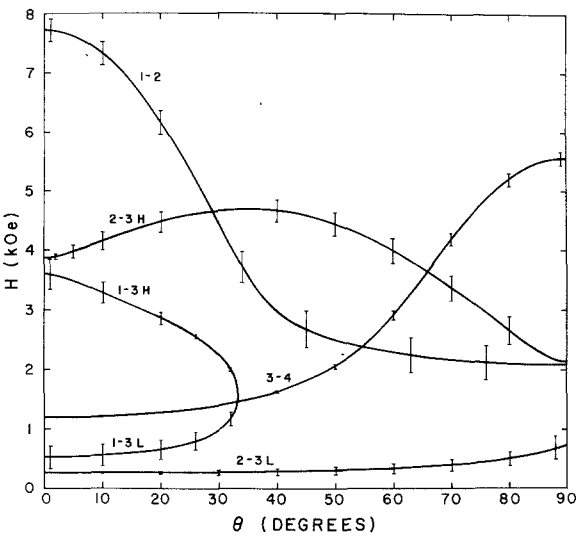

FIG. 5. Isofrequency plot of field vs angle for observable transitions at frequency of 10.0 GHz. Relative transition probabilities indicated.

The student who carried out the computations necessary for the generation of the isofrequency plots of the type shown in Figs. 4 and 5 will find it fascinating to observe the qualitative way in which these plots change as the frequency is varied. At low frequencies, only one or two transitions can be observed, whereas for frequencies much higher than those used for Figs. 4–5, all six possible independent transitions between the various pairs of levels can be observed.

IV. EXPERIMENTAL TECHNIQUE AND RESULTS

A specimen of synthetic single-crystal ruby containing approximately 0.1% chromium was employed in this experiment. Such crystals are readily available from several commercial suppliers at very low cost (less than $1.00 per gram, sometimes free, if optical quality is unimportant). The orientation of the z axis was determined by x-ray techniques to an accuracy of approximately 0.5°. Since what has been called the z axis in this paper is also the optic axis of the optically uni-

axial crystal, this axis can also be determined to within a few degrees by observing the light transmitted through a system of crossed polarizers as the crystal is rotated between the polarizers. In any event, the spectrum itself is employed in making the final determination of crystallographic orientation, as discussed in the preceding section, so that the initial orientation is not an important part of the experiment. The volume of the sample placed within the microwave resonant cavity of the spectrometer is not critical; in the present experiment large resonances were observed with a volume as small as 5 mm^3, although a somewhat larger volume was normally employed. The sample shape is not at all critical, although a diamond saw is useful for preparing a flat surface to facilitate mounting the sample in the cavity.

The measurements reported here were obtained at a frequency of 9.33 GHz, although frequencies from 8.5 through 11.0 GHz have been employed by various groups of students in carrying out the experiment. The frequency was measured with a calibrated cavity wavemeter (0.1% accuracy). As seen in Figs. 4 and 5, a magnetic field as high as 7.5 kOe is required for the observation of all possible transitions at this frequency. The data reported here were obtained using a Harvey–Wells Model L–128 magnet which was much larger than needed for this experiment. It was chosen primarily because the field could be rotated about a vertical axis. Other magnets have been successfully used for this experiment, including magnets which could not be rotated. Almost any magnet capable of a maximum field of 7.5 kOe or greater is suitable. The homogeneity of the field is not as important in this experiment as it would be in an NMR experiment, since the ESR lines are of the order of 20–30 Oe in width.

The accuracy of the results depends upon the accuracy with which the magnetic field can be measured. Although an NMR gaussmeter will provide the greatest possible accuracy, such instruments are inconvenient to use, and they do not have the capability of providing an analog output signal proportional to the magnitude of the field. Consequently, a Hall-effect gaussmeter calibrated to an accuracy of better than 0.5% over the range from zero to 10 kG was employed in obtaining the data reported here. Such gaussmeters are available from several sources, at reasonable cost. In spite of the reduction in accuracy as compared to an NMR gaussmeter, the availability of an electrical signal proportional to the field makes the Hall-effect gaussmeter highly desirable for this type of experiment.

The microwave spectrometer was constructed as simply as possible, and it is depicted schematically in Fig. 6. The resonant cavity was a simple half-wavelength section of rectangular waveguide (TE101 mode), and the sample was glued with Duco cement to one side of the cavity, in such a position that the rf magnetic field was directed vertically throughout the sample. Since the field produced by the magnet was always in the horizontal plane, the two fields were always perpendicular. The klystron source was frequency-stabilized to the resonant frequency of the cavity. This stabilization is essential if resonance signals of reasonable signal-to-noise ratio are to be obtained. Almost any klystron can be used, however, even the very inexpensive 2K25. The ferrite isolator and circulator shown in Fig. 6 are unessential and were used only because they were available. The signals which can be obtained from a ruby sample are so large that almost any sort of spectrometer can be used, and the schematic shown in Fig. 6 is intended merely as a guide. The book by Poole is an excellent source of other spectrometer designs.[10] Two recent papers in this Journal[11,12] describe very simple spectrometers suitable for this type of experiment, making use of recently developed solid-state oscillators. The use of such devices would permit the student starting from "scratch" to construct a suitable spectrometer at very low cost.

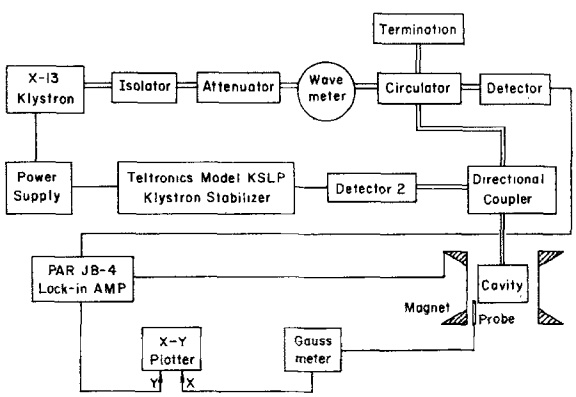

FIG. 6. Schematic block diagram of apparatus.

In order to provide a derivative resonance signal normally employed in ESR experiments requiring higher sensitivity, the magnetic field was modulated at an audio frequency, and the output of the detector was synchronously detected. The resonance data were displayed on an X–Y recorder, with the signal from the gaussmeter applied to one axis and the output of the synchronous detector applied to the other. As will be seen, the data is thereby presented in a form similar to that of the isofrequency plots of Figs. 4 and 5. More accurate measurements could probably have been made, however, by measuring the output of the gaussmeter to higher precision than that obtained with the recorder.

The determination of the exact crystallographic orientation with the ruby sample in the cavity was carried out utilizing the fact that the 2–3H transition exhibits a sharp null in intensity at $\theta=0°$. This rapid variation of the strength of the signal is illustrated in Fig. 7. Here, the resonance absorption is plotted as a function of the magnetic field for several values of the angle θ_M, which represents an arbitrary angular scale reading on the base of the rotatable magnet. The three allowed transitions near 0°, the 1–2, 1–3H, and 1-3L transitions, exhibit nearly constant intensity as θ_M is varied, whereas the small 2–3H transition exhibits a null as θ_M passes through 3°. Thus, when the magnet scale is set to $\theta_M=+3°$, the field is aligned along the crystallographic z axis. It should be noted that the sample was placed into the cavity in such a manner that it was expected that the field would be aligned along the z axis at

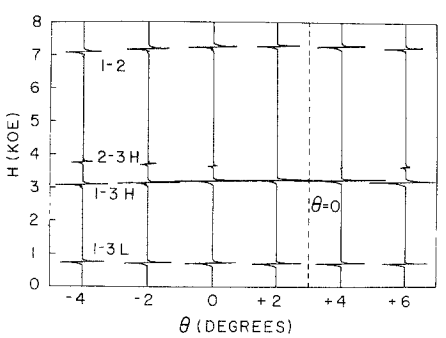

FIG. 7. Experimental ESR data near $\theta=0°$, showing method for determination of direction of z axis by observing the strength of the 2–3 H transition.

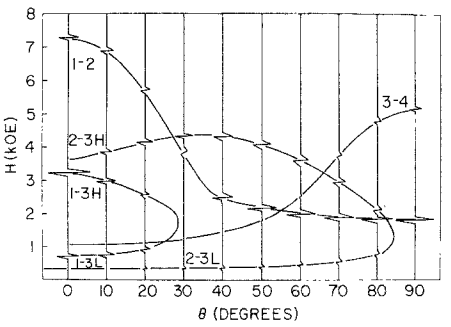

FIG. 8. Experimental isofrequency plot at 9.33 GHz, showing comparison with theoretical curves for $D=5.69$ GHz and $g=1.98$.

$\theta_M=0°$. This difference, amounting to approximately three degrees of misalignment, illustrates the difficulty of maintaining the alignment of a sample in transferring it from, say, an x-ray camera mount to a microwave spectrometer.

Once the orientation of the field with respect to the z axis of the crystal has been determined accurately, the quantities g and D appearing in the spin Hamiltonian can be determined, using the technique outlined in Sec. III. In the present case, using measurements on the three allowed transitions at $\theta=0°$, Eq. (11) gives $g=1.98\pm0.01$ and $D=5.71\pm0.05$ GHz. These values compare quite well with those reported in the literature,[6,9] lying in both cases within the experimental error of the accepted values. Through the use of the X–Y plotter, a good overall impression of the agreement between the experimental data and the calculated positions and intensities of the resonance lines can be obtained, as seen in Fig. 8. In this figure, the observed spectrum is plotted as a function of magnetic field at angles ranging from 0° through 90° at increments of 10°. The curves shown in this figure are those obtained from the spin Hamiltonian, using the values of D and g given above. The calculated transition probabilities are not shown, in order to avoid confusion in this figure, but the measured line intensities may be compared qualitatively with those shown in Figs. 4–5. It should be remembered that the measured intensities represent approximate derivatives of the actual resonance absorption lines. Because of linewidth variations as the direction of the field is varied, the derivative signals do not follow the same quantitative vari-

ation as do the calculated transition probabilities. The qualitative agreement between the calculated transition probabilities and the observed derivative line intensities is, however, quite satisfactory demonstrating quite well the selection rules discussed in the preceding section.

On the whole, the agreement between the experimental results and the theory for the case of ESR in ruby is excellent. Every group of students undertaking this experiment has been able to obtain experimental results of comparable quality. The data can all be obtained in one or two afternoons, after a preliminary session with the instructor to describe the apparatus and its operation. The analysis of the data, particularly the generation of the isofrequency plots of Figs. 4–5, often requires the expenditure of considerable effort on the part of the student, and some students do not wish to carry these computations to completion. Those students (a large majority) who do follow through the computational procedures described in Sec. III and in Appendices II and III invariably find the experience rewarding.

V. CONCLUSION

The experiment described here and its theoretical analysis provide a real challenge to the advanced undergraduate physics student. The student who carries out the complete project, however, has the opportunity, at an early stage in his career, to carry to completion a quantum-mechanical computation and compare his theoretical results with experimental results that he has also obtained himself. That is, he follows the same procedure used by experimental physicists in many areas of research, and he thereby captures the flavor of doing research in a way which is virtually impossible in many types of undergraduate laboratory experiment.

It should be pointed out that the student who reads this paper before carrying out the experiment will miss much of the fun of trying to unravel the meaning of the spectrum. It remains up to the instructor to decide how he wants to guide the student in performing the experiment. On the other hand, it is hoped by the authors that this paper will serve as a useful description of the way in which a fairly difficult experiment has been successfully used in undergraduate education.

APPENDIX I: ENERGY UNITS FOR MAGNETIC RESONANCE

It is usually convenient in any specialized area of research to define special units for such physical quantities as energy or momentum. The choice of units is usually made with a view toward the simplification of calculations or in order that the quantities of interest, when expressed in such specially chosen units, may convey greater meaning. Thus, energy units such as the electron volt and its multiples are commonly used by nuclear and elementary-particle physicists. In the case of magnetic resonance, energy differences between levels are measured by observing resonant transitions between such levels under excitation with radiation at a definite frequency. It is, therefore, natural to express energy in terms of frequency units when dealing with such problems, since such units make the calculations involved in the computation of transition frequencies simpler. Furthermore, if quantities such as the zero-field-splitting parameter D are expressed in frequency units, it is often a simple matter to estimate roughly what transitions of a particular system can be excited at a given frequency.

With regard to the Zeeman Hamiltonian, it is convenient to express the value of the Bohr magneton as $\mu_B = 1.3997$ GHz/kOe. Then, with the field expressed in kilo-Oersteds, the Zeeman energy is expressed also in frequency units.

APPENDIX II: SOLUTION OF SECULAR EQUATION AND CALCULATION OF EIGENVECTORS

The secular equation given in Eq. (16) can be written as a simple quartic equation whose coefficients are functions of the magnitude and direction of the magnetic field. Although a quartic equation can be solved algebraically, it is more convenient in the present case to employ the Newton–Raphson method for the numerical solution of the roots of the equation. Since a computer is required for the efficient generation of the isofrequency plots of interest in the present case, the use of a purely numerical iterative solution for the roots of the secular equation is not a particular problem. The main purpose of this

Appendix is to point out that the most efficient use of the Newton–Raphson iterative method for finding the roots of the equation can be made if an intelligent choice of a starting approximation for the roots is made. In the present case, two of the roots can be found efficiently by starting the iteration at the inflection points of the quartic equation. The remaining roots can be quickly found by solving the quadratic equation which is obtained by factoring the quartic once the first two roots have been found. A FORTRAN program can be written in less than 20 statements to solve for all four roots of the secular equation. Although general programs are available for obtaining the roots of polynomials, it is good practice for the beginning student to write his own program in this particularly simple case.

Once the roots of the secular equation have been found, the coefficients A_{nm} of the eigenvectors can be computed by any of several techniques. Again, general computer programs are available for such calculations, but it is worthwhile for the student to write his own. The simplest method, although it is not mathematically elegant, is to assume that one of the coefficients is different from zero and then to solve three of the four simultaneous equations which make up the complete matrix eigenvalue equation for the remaining three coefficients. This procedure, which must be repeated for each energy eigenvalue, is full of pitfalls for the unwary student, but it is the procedure chosen most often. Actually a completely trouble-free program totaling fewer than 35 FORTRAN statements can be written to calculate all sixteen coefficients A_{nm}.

APPENDIX III: COMPUTATION OF ISOFREQUENCY PLOTS

As pointed out in Sec. III, the results of the theoretical computation of the eigenvalues of the spin Hamiltonian are most effectively displayed in terms of an isofrequency plot such as those shown in Figs. 4–5. It is the purpose of this Appendix to describe a simple method for the generation of such plots. The method is only briefly outlined here, since each student who undertakes this type of project will undoubtedly wish to work out the details of the method for himself.

Consider the quartic function whose roots are the energy eigenvalues of the spin Hamiltonian to be a function of both the energy and the magnetic field. The secular equation can then be written in the symbolic form $F(E, H) = 0$. This equation defines an implicit relationship between the energy and the magnetic field, and, although the roots of a polynomial are not analytic functions of the coefficients of the polynomial, it is possible, using straightforward techniques from calculus, to obtain an algebraic expression for the derivative of the energy with respect to the value of the applied magnetic field. It is, then, quite a simple matter to employ a method employing the Newton–Raphson technique to find the exact value of the magnetic field at which a particular transition will occur at a given frequency.

* Supported in part by the National Science Foundation.

[1] R. E. Norberg, Am. J. Phys. **33,** 71 (1965).

[2] P. J. Limon and R. H. Webb, Am. J. Phys. **32,** 361 (1964).

[3] C. P. Slichter, *Principles of Magnetic Resonance* (Harper and Row, New York, 1963).

[4] G. E. Pake, *Paramagnetic Resonance* (Benjamin, New York, 1962).

[5] C. P. Poole and H. A. Farach, *The Theory of Magnetic Resonance* (Wiley, New York, 1972).

[6] A. Abragam and B. Bleaney, *Electron Paramagnetic Resonance of Transition Ions* (Oxford, New York, 1970).

[7] A. Melissinos, *Experiments in Modern Physics* (Academic, New York, 1966).

[8] R. B. Leighton, *Principles of Modern Physics* (McGraw–Hill, New York, 1957).

[9] E. O. Schulz-Dubois, Bell Syst. Tech. J. **38,** 271 (1959).

[10] C. P. Poole, *Electron Spin Resonance* (Wiley, New York, 1967).

[11] L. W. Rupp, W. M. Walsh, and A. Steinfeld, Am. J. Phys. **38,** 238 (1970).

[12] F. K. Manasse and E. W. Kyllonen, Am. J. Phys. **40,** 1171 (1972).